Proceedings of the
4th JSME-KSME Thermal Engineering Conference
October 1-6, 2000, Kobe, Japan

I307

OBSERVATION OF LIQUID JET DISINTEGRATION UNDER DC AND AC/DC-COUPLED ELECTRIC FIELDS

Myoung Chan Kim and Sang Yong Lee

Department of Mechanical Engineering
Korea Advanced Institute of Science and Technology
373-1, Kusong-dong, Yusong-gu, Taejon 305-701, Korea

ABSTRACT To obtain fine uniform liquid drops ranging between 30 to 200 microns, a series of tests were performed by applying the DC and AC/DC-coupled electric fields to the discharged liquid jet. For the liquid with the electric conductivity larger than 10^{-7} S/m such as water, discharging with the spindle mode turned out to be the only way to generate the drops within this size range. The drops become smaller and relatively uniform when the DC voltage is applied, and there was the optimum voltage input for each liquid flow rate. This optimum voltage increases with the higher liquid flow rate. When the AC power is superposed on the DC voltage input, the liquid-column (spindle) length becomes more regular, and accordingly the drops become more uniform.

Keywords: AC/DC-coupled electric fields, Optimum voltage, Spindle mode

1. INTRODUCTION

When the liquid jet is exposed to a strong electric field, it tends to be disintegrated into small drops. This type of liquid disintegration is often termed as the electrohydrodynamic atomization since the liquid jet is disintegrated both by the electric and hydrodynamic forces. When the high-voltage electricity is applied, not only the smaller drops are obtained but also the flight paths of the atomized drop can be controlled. The technique of electrohydrodynamic atomization has variety of applications. It can be applied to the spray painting [1,2], spraying of insecticide [3] and liquid metals [4], ink-jet printing [5], formation of colloidal particles [6] or powders [7, 8], fuel spraying [9,10], thin-film formation [11, 12], and the emission control [13, 14].

Table 1 shows the liquid disintegration modes when the strong DC or AC/DC-coupled electric field is applied. The uniform-size drops less than 10 microns can be obtained when a high DC-voltage is applied to a bulk liquid, but with an extremely small flow rate. This type of flow is denoted as the cone jet mode and the drop sizes are independent of the nozzle hole diameter. The size uniformity of drops can be improved by coupling the AC power to this DC power. On the other hand, uniform drops larger than 300 microns can be obtained by dripping the liquid with somewhat higher liquid flow rate under DC electric field, and the uniformity can be improved under the AC/DC-coupled electric field. With the further increase of flow rate, a simple solid jet is formed, but in this case, the monodisperse drops larger than 200 microns can be easily obtained under the AC/DC-coupled electric field. It should be noted that the drop sizes by both the dripping and the simple jet modes depend strongly on the nozzle hole diameter. The smaller and uniform drops may be obtained with the smaller hole-size; however, it is impractical to make the hole diameter smaller than about 200 microns. Thus, with the AC/DC coupling technique, the uniform

Table 1 Formation of drops under DC or AC/DC-coupled electric field

Mode		Cone Jet	Micro-dripping	Spindle		Simple Jet	Dripping
Average Dropsize[μm]		Less than 10	10~200	30~200	200~450	More than 200	More than 300
Size Distribution	DC	Mono-disperse[15]	Relatively Uniform[16]	Disperse[16]		Widely Disperse[16]	Mono-disperse[16]
	AC/DC	Improved	Not Reported	Not Reported	Improved[17]	Mono-disperse[18]	Improved[19]

drops larger than about 200 microns could be obtained at most. On the other hand, there are very little works reported on the generation of the mono-dispersed drops raging from 10 to 200 microns. The work by Cloupeau and Prunet-Foch[16] is the only one available to the authors' knowledge. Relatively uniform drops may be obtained with the microdripping mode under the DC electric field, but occurrence of this mode strongly depends on the nozzle-tip shape and the wettability between the liquid and the nozzle surface. With the microdripping mode, single droplets are formed from a liquid apex. The electric conductivity of the liquid is also one of the factors influencing the occurrence of this mode. For example, the microdripping phenomenon was not observed with when the water was used. Thus, in the present study, the technique of applying the AC/DC-coupled electric field was tried to see if it is feasible to obtain the monodisperse drops within the range of 30-200 microns.

2. EXPERIMENTS

Figure 1 shows the configuration of the experimental setup for the electrohydrodynamic atomization. The system basically consists of the liquid supply and the high-voltage supply parts. A syringe pump(Orion, model 305) was used for the accurate supply of the liquid ranging from 1×10^{-5} to 1×10^{-1} ml/s. To apply a high-voltage DC electricity, a high-voltage DC-power supply (KSC Co., 30 kV, 5 mA max.) was used. For AC/DC-coupled experiments, the DC-power supply was connected to a high-voltage AC-power supply (KSC Co., 15 kV peak-to-peak voltage, 10 mA max., 20 – 2000 kHz). A high voltage probe (Tektronix, Model 6015A) was used to measure the voltage between the nozzle tip and the ground electrode separated by 8 mm in axial direction in the present experiment. The ground electrode has a hole of 15 mm at the center through which the liquid jet or drops pass by. A resistance of 10 MΩ was connected between the ground electrode and the earth to avoid the current overflow when the electric spark occurs. The needle-type nozzle is made of the stainless steel (SUS 304) tube with its inner and outer diameters being 0.13 and 0.3 mm, respectively. The ultra pure water with the electric conductivity of 1.5×10^{-4} S/m was used as the test fluid. The instantaneous configuration of the liquid discharge was visualized and recorded by a black and white CCD camera (Toshiba, Model NB.1K537K) along with a strobo-light of 10 microsecond flash duration and a microcomputer. In addition, in order to see the formation of the liquid column consecutively, a high speed video camera (Kodak Ektapro hi-spec Motion analyzer, Model 1000-E) was used. The recording rate of this video camera is 12000 frames/sec and the image frame resolution is 256×192. A PMAS(particle motion analyzer system, V-Tek) was used to measure the drop size distribution of the spray. The discharge current between the nozzle and the ground electrode (Cu plate) is measured using a multimeter(HP 3458A).

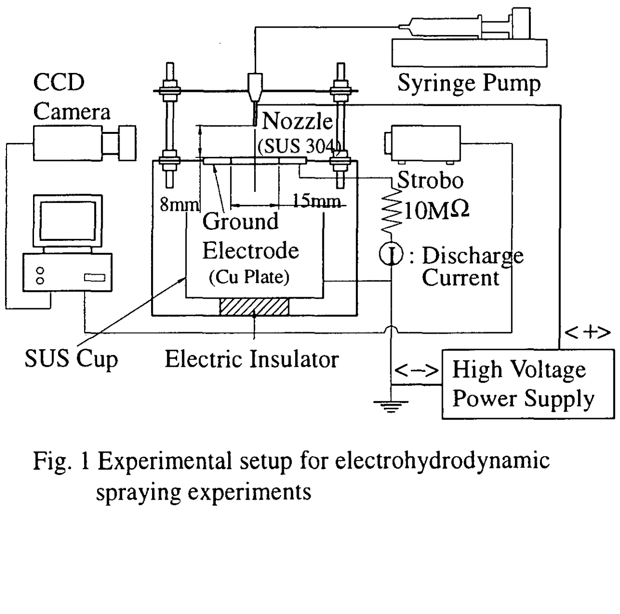

Fig. 1 Experimental setup for electrohydrodynamic spraying experiments

3. RESULTS AND DISCUSSION

At the first stage of the present experiment, the effects of the liquid flow rate and the DC input voltage on the formation of drops were examined. As in Fig. 2, various modes are observed with different DC voltages for a fixed liquid flow rate (1.04×10^{-4} ml/s). When the input voltage is low (Fig. 2(a) and (b)), a drop with its size much larger than the nozzle inner diameter is formed, and it is known to be the dripping phenomenon. When the voltage is raised to 4 kV, a thin liquid column is formed and from that, a small drop is formed (Fig. 2(c)); this mode is known as the spindle mode. In the spindle mode, the droplets are formed either by the liquid jet breakup or directly by the detachment of the liquid volume accumulated in the meniscus. The detached liquid volume may form a single drop or break up into several droplets. If the voltage is more increased (above 6 kV), a longer liquid column is observed,

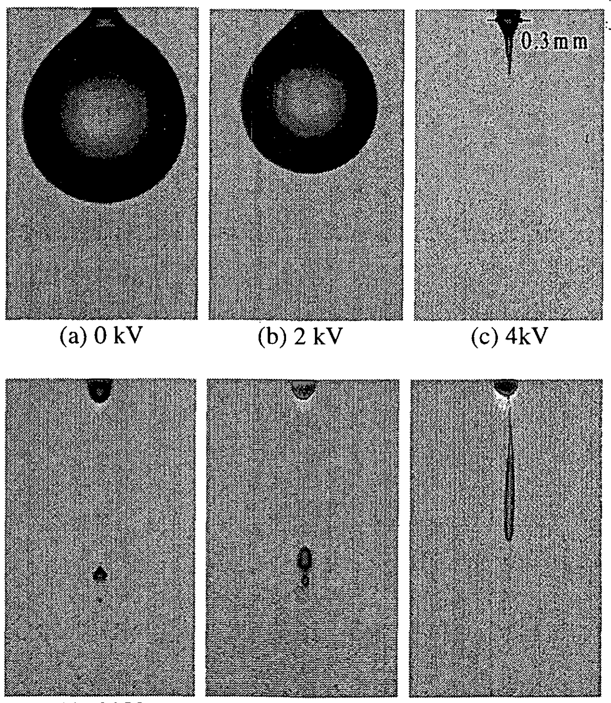

(a) 0 kV (b) 2 kV (c) 4kV

(d) 6 kV (e) 8 kV (f) 10 kV

Fig. 2 Change of the drop generation mode with the voltage input (Liquid flow rate: 1.04×10^{-4} ml/s) and accordingly, the drop size becomes larger. In this mode, though the drop size is large, the diameter of the liquid column is still smaller than the nozzle inner diameter, and it is termed here "elongated spindle mode". With the elongated spindle mode, a glow corona is formed at the at the nozzle tip due to the ionization of the ambient air. This space charge reduces the strength of the electric field, and opposes the disintegration of the liquid column. Hence, the spindle mode is considered to be the optimum mode to obtain the fine spray drops.

A map of the drop formation modes was constructed as Fig. 3 with the liquid flow rate and the DC voltage input taken as its axes. Dripping occurs at the low-voltage (below 3.5 kV) with the low-flow rate (below 0.03 ml/s) condition in the right-hand side of the figure. The simple jet mode is seen at the higher flow rate condition. The spindle mode appears approximately between the ranges 3.5 – 5.5 kV and 10^{-5} – 10^{-2} ml/s. In the same figure, the conditions for the formation of the glow corona are indicated as the solid dots; the glow corona bounds the upper region of the spindle mode.

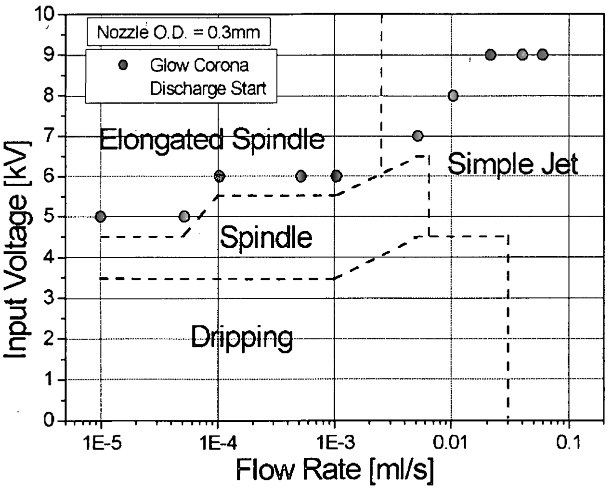

Fig. 3 Classification of the drop generation mode (DC electric field)

Since the spindle mode is thought to be the desirable atomization mode, the drop sizes were measured in this region to see the effect of the flow rate and the DC voltage input on the atomization performance in detail. Figure 4 shows the examples of the volume-based size histogram of the spray drops formed with different values of the DC voltage input for the spindle mode. At least 1000 drops were sampled to obtain each distribution and the measurement error stays within $\pm 10\%$. With the low voltage input (Fig. 4(a)), it can be easily confirmed that most of the discharged liquid is converted into large drops around 150 microns. In this case the SMD value is measured to be 148.3 microns. However, with the higher input voltage, those drops break down to smaller ones (Fig. 4(b)) and the SMD value is measured to be 36.5 microns. If the voltage input is further increased, due to the stronger space charge, the atomization quality becomes somewhat poor(Fig. 4(c)). In other words, a considerable number of the large drops are still unatomized, and the SMD value appears to be 43.6 microns which is larger than the case of Fig. 4(b).

The time elapsed between the generations of one ligament and that of the next one is measured by a high speed video camera. Figure 5 shows the probability density distribution of the ligament generation frequency from these data points. Average frequency increases as the voltage input changes from 3.5kV to 3.75kV (See Figs. 5 (a) and (b)). However, when the voltage input is raised from 3.75kV to 4.0kV, two frequency bands are observed with one of them at the low frequency range as in Fig. 5 (c). The ligament generation in the low frequency range results in formation of large drops as confirmed in Fig. 4 (c). Concerned with the formation of the positive corona, the burst pulse corona shows up in the low voltage input condition and then the streamer corona, glow corona,

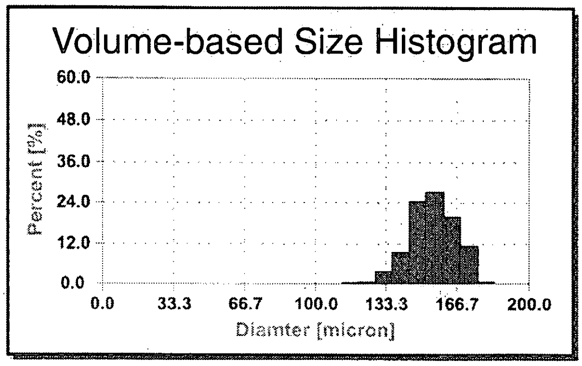

(a) DC: 3. 50kV, SMD=148.30μm

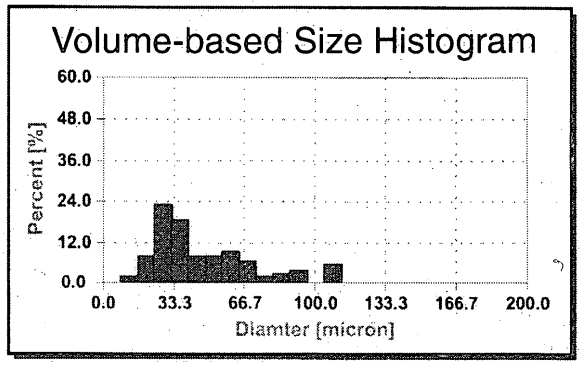

(b) DC: 3. 75kV, SMD=36.50μm

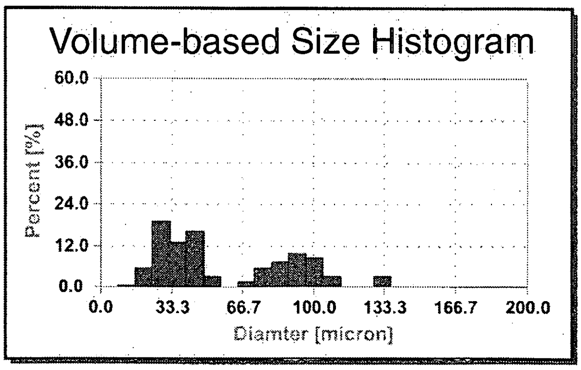

(c) DC: 4. 00kV, SMD=43.60μm

Fig. 4 Variation of the drop size distribution with the DC voltage input (Liquid flow rate: 1.04×10^{-4} ml/s)

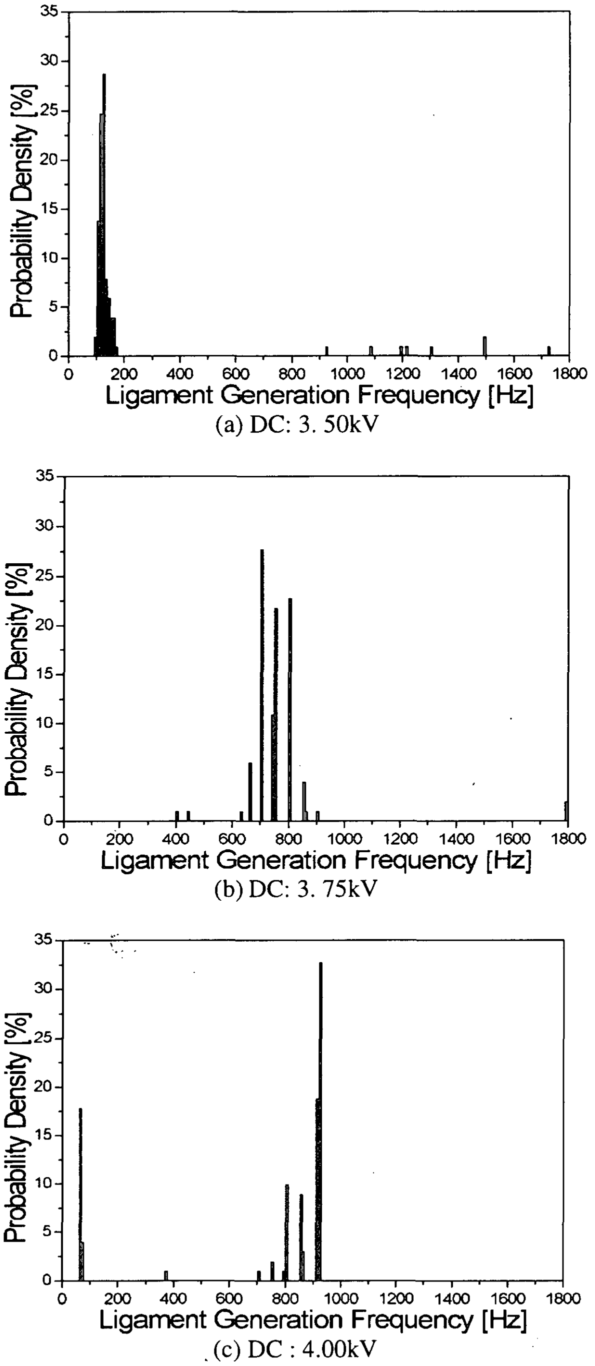

(a) DC: 3. 50kV

(b) DC: 3. 75kV

(c) DC : 4.00kV

Fig. 5 Dependence of the probability density distribution of the ligament generation frequency on the DC voltage input (Liquid flow rate: 1.04×10^{-4} ml/s)

and spark discharge appear consecutively as the input voltage increases. Among them, the burst pulse or the streamer corona discharge occurs in the spindle mode. As the DC-voltage input is raised, the strength of the electric field generally increases. However, the occurrence of the space charge due to the corona discharge disturbs the electric field and reduces the strength of the electric field eventually. Hence, there is an optimum voltage input for

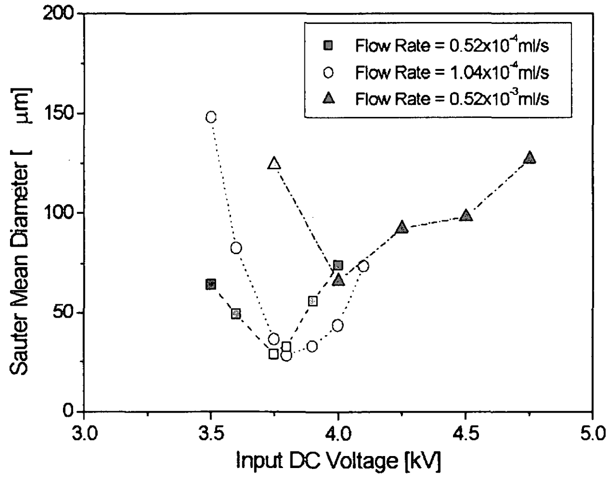

Fig. 6 Variation of SMD with the DC voltage input

regular generation of the ligaments, and hence, the drops (Fig. 4 (b)).

To summarize this trend, the variations of SMD with the voltage input for different liquid flow rates were plotted as in Fig. 6. There is obviously a minimum drop size for each flow rate condition, and the minimum SMD occurs at the higher input voltage when the liquid flow rate is increased. This is because, the more electricity is needed to disintegrate the same amount of the liquid.

Figure 7 shows the discharge current through the ground electrode with the change of the input voltage. Here, the sampling duration is 16.7 ms and the sampling interval is 45.0 ms. The data points shown in Fig. 7 are the averages of 2000 measurements made for each experimental condition and the error bars represent the ranges of the measured data. The inception of the current discharge occurs earlier with the higher liquid flow rate (See point A, B, C in Fig. 7). This is because the effective distance between the electrode (the distance between the breakup point of the liquid column and the ground electrode)

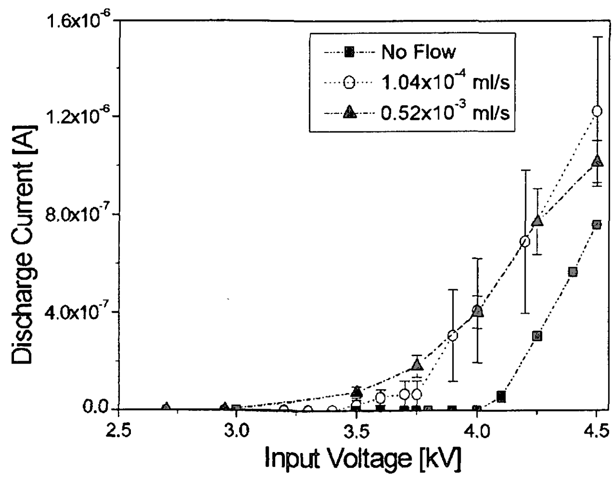

Fig. 7 Variation of the average discharge current through the ground electrode with the DC voltage input

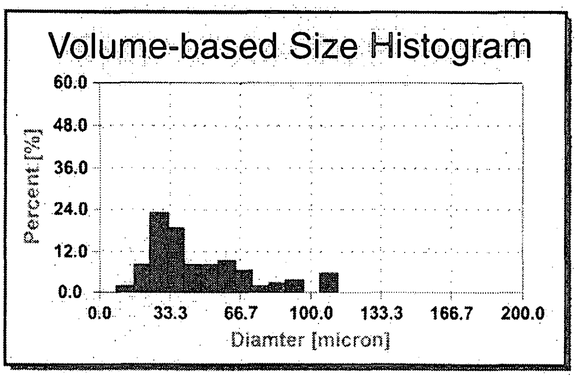

(a) DC: 3. 75kV, SMD=36.50μm

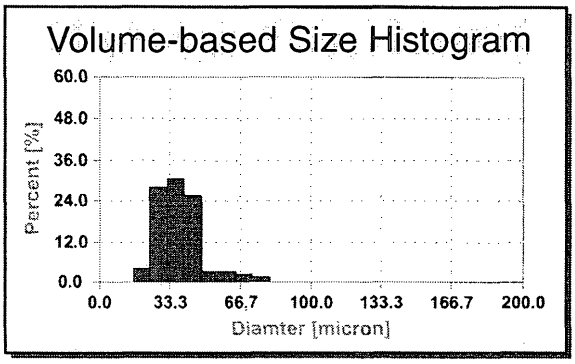

(b) AC/DC : 3. 75kV± 0.63kV$_{pp}$, 500Hz, SMD=34.49μm

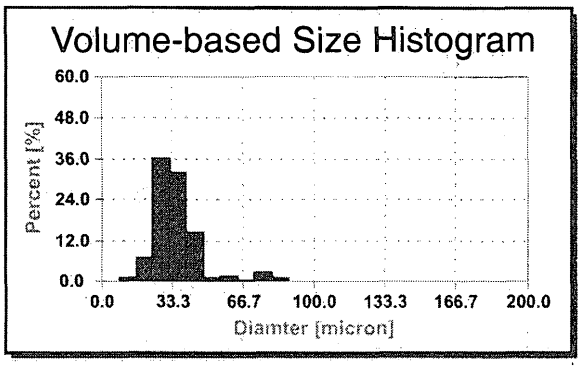

(c) AC/DC : 3. 75kV± 0.31kV$_{pp}$, 500Hz, SMD=31.74μm

Fig. 8 Effect of the AC electricity on the drop size distribution
(Liquid flow rate: 1.04×10^{-4} ml/s)

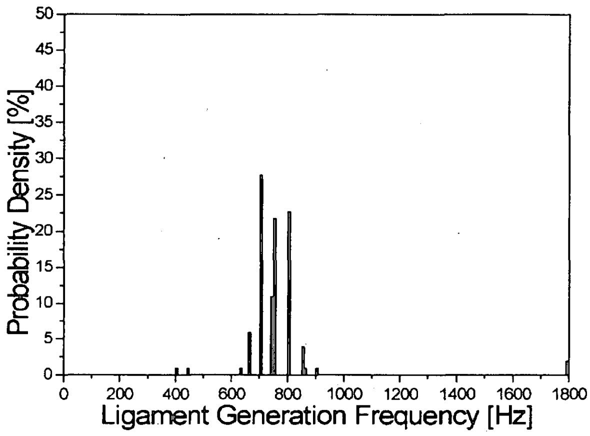

(a) DC : 3.75kV

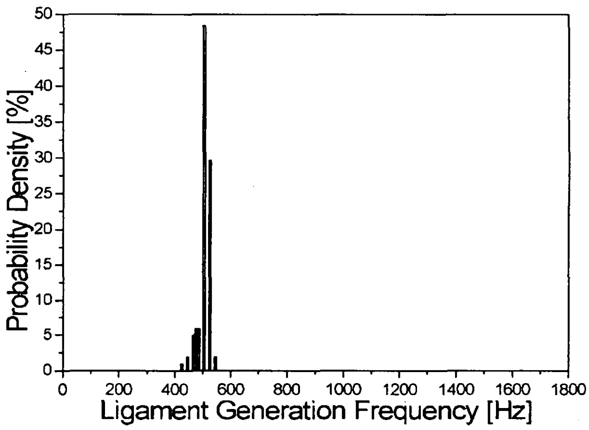

(b) AC/DC : 3. 75kV± 0.63kV$_{pp}$, 500Hz

Fig. 9 Effect of the AC electricity on the probability density distribution of ligament generation frequency
(Liquid flow rate: 1.04×10^{-4} ml/s)

becomes closer. Above these inception points, the discharge current increases sharply and also the fluctuation becomes large. For a given flow rate, the electric-field strength increases with the input voltage, and the drop size decreases accordingly, as seen in Fig. 6. At the same time, the discharge current starts to fluctuate as shown in Fig. 7 and keeps growing with the input voltage. This degrades the atomization quality and the drop size increases beyond the minimum SMD condition as in Fig. 6.

At this stage, it is meaningful to see the effect of the AC electricity on the atomization performance of the nozzle. In the present experiment, An AC power was superposed with the DC power, and the frequency of the AC power was changed from 100 Hz to 2000 Hz with every 100 Hz intervals. Also, for peak-to-peak values of the AC voltage, two different fractions (1/6 and 1/12) of the DC voltage input were tested. Figure 8 shows examples of the AC voltage effect: here, the AC Frequency, DC voltage and the liquid flow rate were fixed to be 500 Hz, 3.75 kV and 1.04×10^{-4} ml/s, respectively. With the superposition of the AC power, the drop sizes become uniform as can be compared between Fig. 8 (a) and (b). However, at present, it is yet hard to tell the effect of the peak-to-peak voltage of the AC power on the atomization performance (characteristics). (See Fig. 8 (b) and (c).)

When the AC power is superimposed to the DC power, the generation of the liquid column becomes more regular, and accordingly the drops become more uniform. Figure 9 confirms the generation of the liquid ligament under the AC/DC-coupled field is more regular (i.e. narrower frequency band of ligament generation) compared with that under the DC-only field.

4. CONCLUSION

In the present study, a series of tests were performed to obtain the small-sized uniform liquid drops ranging between 30 to 200 microns by applying the DC and AC/DC-coupled electric fields to the discharging liquid jet. For the liquid with the electric conductivity larger than 10^{-7} S/m (such as water), operating the system with the spindle mode is considered to be the only way to generate the drops within this size range. The drops become smaller and relatively uniform when the DC voltage is applied, and there was the optimum voltage input for each liquid flow rate. This optimum voltage increases with the higher liquid flow rate. When the AC power is superposed with the DC power, the generation of the spindle becomes more regular, and accordingly the drops become more uniform.

5. ACKNOWLEDGEMENTS

The present work was supported by the National Research Laboratory Program and partly by the Brain Korea 21 Project. This work was performed also under the auspices of Korea Science and Engineering Foundation (KOSEF, 98-0200-03-01-2, 98-2-09-04-01-2).

6. REFERENCES

1. Hines, R. L., Electrostatic Atomization and Spray Painting, J. Appl. Phys., Vol.37, No.7 (1966), pp.2730-2736.
2. Snyder, H. E., Senser, D. W., Lefebver, A. H. and Coutinho, R., S., Drop size Measurements in Electrostatic Paint Sprays, IEEE Trans. Ind. Appls., Vol. 25, No. 4 (1989), pp.720-727.
3. Abdel-Salam, M. S., Soliman, F. A. and Mgahed, A. A., Electrostatic-Based Pesticide Spray Systems. part 1 : a Theoretical Investigation, J. Phys. D:Appl. Phys., Vol 26 (1993), pp.2082-2091.
4. Lohmann, M., Beyer, H. and Schmidt-Ott, A., Size and Charge Distribution of Liquid Metal Electrospray Generated Particles, J. Aerosol Sci., Vol. 28 (1997), pp.s349-s350.
5. Atten, A. and Oliveri, S., Charging of Drops Formed by Circular jet Breakup, J. Electrostatics, Vol. 29 (1992), pp.73-91.
6. Kidd, P. W., Parametric Studies with a Single-Needle Colloid Thruster, J. Spacecraft, Vol. 5, No. 9 (1968), pp.1034-1039.
7. Borra, J-P., Camelot, D., Marijinissen, J. C. M. and Scarlett, B., A new Production Process of powders with Defined Properties by electrohydrodynamic Atomization of Liquids and Post-production Electrical Mixing, J. Electrostatics, Vol. 40&41 (1997), pp.633-638.
8. Fu, D., Processing of Porcelain Enamel Glass Powders for Electrostatic Spraying, Powder Technolgy, Vol. 85 (1995), pp.65-69.
9. Djuric, Z., Balachandran, W. and Wilson, C. W., Electrical Field and Space Charge Modelling in a Viscous Fluid Flow in a Nozzle, J. Phys. :Appl. Phys., Vol. 31(1998), pp.2132-2144.
10. Shrimpton, J. S., Yule, A. J. and Watkins, A. P., Performance Data of an Electrostatic Atomizer for Highly Resistive Liquids, Proc. of ICLASS-`97 (1997), pp.625-632.
11. Hoyer, B., Sorensen, G, Jensen, N., Nielsen, D. B. and Larsen, B., Electrostatic Spraying : A Novel Technique for preparation of Polymer Coatings on Electrodes, Anal. Chem. Vol. 68 (1996), pp.3840-3844.
12. Zomeren, A. A. V., Kelder, E. M., marijnissen, J. C. M. and Schoonman, J., The Production of Thin Films of $LiMn_2O_4$ by Electrospraying, J. Aerosol Sci., Vol. 25, No. 6 (1994), pp.1229-1235.
13. Bellan, J. and Harstad, K., Mechanical and Electrostatic Dispersion of a Polydisperse Cluster of Drops for Soot Control, Proc. of ICLASS-'97 (1997), pp.617-624.
14. Wang, S. H., Chang, J. S. and Berezin, A. A., Atomization Characteristics of Electrohydrodynamic Limestone-water Slurry Spray, J. Electrostatics, Vol. 30 (1993), pp.235-246.
15. Cloupeau, M., Recipes for Use of EHD Spraying in Cone-jet Mode and Notes on Corona Discharge Effects, J. Aerosol Sci., Vol. 25, No. 6 (1994), pp.1143-1157.
16. Cloupeau, M. and Prunet-Foch, B., Electrostatic Spraying of Liquids: Main Functioning Modes, J. Electrostatics, Vol. 25 (1990), pp.165-184.
17. Sample, S. B. and Bollini, R., Production of Liquid Aerosols by Harmonic Electrical Spraying, J. Colloid and Interface Sci., Vol. 41, No,. 2 (1972), pp.185-193.
18. Huneiti, Z., Balachandran, W. and Machowski, W., The Study of AC Coupled DC Fields on Conducting Liquid Jets, J. Electrostatics, Vol. 40, No. 41 (1997), pp.97-102.
19. Balachandran, W., Machowski, W. and Ahmad, C. N., Electrostatic Atomization of Conducting Liquids using AC Superimposed on DC Fields, IEEE Trans. Ind. Applics., Vol. 30, No. 4 (1994), pp.850-855.

7. NOMENCLATURE

AC : alternating current
DC : direct current

Subscript
pp : peak-to-peak value